ELSEVIER

Biochemical Pharmacology 62 (2001) 893–902

Biochemical Pharmacology

Early effects of AZT on mitochondrial functions in the absence of mitochondrial DNA depletion in rat myotubes

Ornella Cazzalini[a,*], Maria C. Lazzè[a], Luisa Iamele[a], Lucia A. Stivala[a], Livia Bianchi[a], Patrizia Vaghi[b], Antonia Cornaglia[b], Alberto Calligaro[b], Daniela Curti[c], Andrea Alessandrini[d], Ennio Prosperi[e], Vanio Vannini[a]

[a]*Dipartimento di Medicina sperimentale, sez. Patologia generale «C. Golgi», P.zza Botta 10; I-27100 Pavia, Italy*
[b]*sez. Istologia e Embriologia generale, via Forlanini 10, I-27100 Pavia, Italy*
[c]*Dipartimento di Scienze Fisiologiche e Farmacologiche cellulari e molecolari, P.zza Botta 11, Università di Pavia, I-27100 Pavia, Italy*
[d]*INFM, Dipartimento di Fisica, Centro di Microscopia elettronica, via Irnerio 46, Università di Bologna, I-40126 Bologna, Italy*
[e]*Centro di studio per l'Istochimica del CNR, P.zza Botta 10, Università di Pavia, I-27100 Pavia, Italy*

Received 15 December 2000; accepted 7 May 2001

Abstract

Zidovudine (AZT) is a potent inhibitor of human immunodeficiency virus (HIV) replication. In humans, as well as in animal models, long-term treatment with AZT induces a severe myopathy characterised by structural and functional alterations of mitochondria associated with depletion of mitochondrial DNA (mtDNA). In the present work, we compared the effects induced by AZT on mitochondria upon short- or long-term treatments of cultured rat myotubes. Morphological alterations were investigated by electron microscopy, and mtDNA depletion and deletions were analysed by Southern blot. Mitochondrial membrane potential was determined after JC-1 staining by laser-scanning confocal microscopy in whole cells, and by flow cytometry in isolated muscle mitochondria. We found that the early effects of AZT on mitochondrial functions were a marked, yet reversible reduction in mitochondrial membrane potential, in the absence of any effect on mtDNA. The long-term treatment, in addition to mitochondrial membrane potential alterations, induced morphological changes in mitochondria, and a remarkable reduction in the amount of mtDNA, without any significant evidence of mtDNA deletions. In both treatments, a block of the spontaneous contraction of myotubes was observed. To study in more detail the early effects induced by AZT, the ability of the drug to interact with cardiolipin, an important component of internal mitochondrial membrane, was investigated by atomic force microscopy (AFM) in an artificial membrane model system. The results suggest that the primary effects of AZT may be related to a physical interference with the membrane structure leading to a consequent modification of its physical characteristics.

Keywords: Zidovudine; Myotubes; JC-1; Laser-scanning confocal microscopy; Atomic force microscope; mtDNA

1. Introduction

Zidovudine (3′-azido-2′, 3′-dideoxythymidine; AZT) is a potent inhibitor of human immunodeficiency virus (HIV) replication. The antiretroviral activity of AZT was found to derive from its conversion into AZT triphosphate, which inhibits HIV-1 reverse transcriptase by terminating the newly synthesized viral DNA chain [1]. Unfortunately, patients treated with AZT develop a toxic mitochondrial myopathy [2–6]. Typical morphological features of this myopathy are the formation of ragged-red fibres and various mitochondria abnormalities, including enlarged size and abnormal cristae [3]. Mitochondrial ultrastructural changes were also detected in AZT-treated animals [7–10] and in human or mouse muscle cell cultures [11,12]. In humans, in animal models, as well as in different human cell lines, mtDNA depletion was also observed [8,9,12,13]. Thus, mtDNA replication has been considered the first mitochondrial target to explain the toxic effect of AZT. It has been demonstrated that mtDNA depletion is dependent on the

* Corresponding author. Tel.: +39-382-506-333; fax: +39-382-303-673.
E-mail address: ornella@manuzio.unipv.it (O. Cazzalini).

Abbreviations: AZT, zidovudine; mtDNA, mitochondrial DNA; AFM, atomic force microscopy; JC-1, 5,5′,6,6′-tetrachloro-1,1′,3,3′-tetraethylbenzimidazolylcarbocyanine iodide; SDH, succinate deydrogenase; COX, cytochrome oxidase; and PCR, polymerase chain reaction.

0006-2952/01/$ – see front matter
PII: S0006-2952(01)00713-4

inhibition of DNA polymerase γ, the matrix enzyme responsible for mtDNA synthesis [14,15]. An alternative proposal to explain the biochemical origin of mtDNA alteration is the massive conversion of guanosine into 8-OH-guanosine induced by AZT [10,16].

The long-term AZT treatment has been shown to induce mitochondrial biochemical dysfunction in AIDS patients, rats and isolated cells [3,9,17–21]. Some biochemical alterations were also reported in mitochondria after short-term AZT treatment [18]; in particular, we previously reported membrane potential abnormalities, both in isolated mitochondria treated with AZT *in vitro* and in mitochondria isolated from long-term AZT-treated rats [9].

The aim of the present study was to analyse the effects induced by AZT after short- and long-term treatments, using primary cultures of rat myotubes. Morphological, biochemical, and mtDNA alterations were investigated. Mitochondrial membrane potential modifications, as determined with the fluorescent probe 5,5′,6,6′-tetrachloro-1,1′,3,3′-tetraethylbenzimidazolylcarbocyanine iodide (JC-1), were assessed in rat isolated muscle mitochondria by flow cytometric analysis, and in rat myotube cultures by laser-scanning confocal microscopy.

In isolated mitochondria, the flow cytometric analysis showed an immediate alteration in mitochondrial membrane potential associated with a reduction in SDH activity. In cultured myotubes, the results showed that 72-hr AZT treatment induced a dramatic, though reversible, reduction in mitochondrial membrane potential, in the absence of any effect on mtDNA. The three-week treatment, in addition to mitochondrial membrane potential alterations, induced morphological changes in mitochondria and a remarkable reduction in the amount of mtDNA, without any significant evidence of mtDNA deletion. In both treatment schedules, a decrease in SDH activity and a block of the spontaneous contraction of myotubes were observed. AFM analysis of AZT on cardiolipin crystalline structure suggests the possibility that AZT interacts with the structure of mitochondrial membrane. The alteration of membrane potential caused by AZT is thought to be related to a reversible physical effect of this molecule on the structural organization of the membrane, with consequent modification of its physical characteristics.

2. Materials and methods

2.1. Cell culture and treatments

2.1.1. Isolation of satellite cells

Satellite cells (myoblasts) were isolated as described by Pinset and Montarras [22] from gastrocnemius, extensor digitorum leg and soleum of male Wistar rats (Harlan Nossan, weight 100–150 g) by sterile dissection. All tissue were thinly minced in PBS and then digested in MCDB 104 medium (GIBCO, BRL) containing 0.1% w/v trypsin (Sigma) and 0.05% w/v collagenase–dispase (Boehringer Mannheim). The digestion was performed by 5 successive 5-min incubations at 37° with gentle shacking. After proteolytic digestion, the cell suspensions were filtered through a sterile nylon gauge, collected by centrifugation, and seeded on Petri dishes to allow adherence of contaminating fibroblasts in proliferation medium [for 100 mL: Dulbecco's modified Eagle's medium (DMEM, GIBCO) 40 mL, MCDB 104 (GIBCO) 40 mL, Ultroser G (GIBCO) 2 mL, fetal bovine serum (FBS) 20%, 100 IU/mL of penicillin, 100 μg/mL of streptomycin].

2.1.2. Myotube culture

After 24 hr, the suspension cells were shifted to collagen-coated (collagen type I, Sigma) flask or coverslip to allow adherence and proliferation of myoblasts. The colonies were grown in proliferation medium for 10 days. At this time, differentiation was induced by DMEM and MCDB 104 medium 1/1, supplemented with 10% FBS and antibiotics. Myoblast growth and development of myotubes were followed by daily microscopic examinations under an inverted microscope. When the cultures were enriched in myotubes, usually after two weeks, 2 mg/mL (7.4 mM) for short-term treatment or 0.2 μg/mL (740 nM) for long-term of AZT (Burroughs Wellcome) were added to flasks or coverslips. The last dose corresponds to the high daily dose used in the treatment of AIDS. The cultures treated with 2 mg/mL of AZT were processed for confocal microscopical analysis after 4, 24, 48, or 72 hr treatment and for mtDNA depletion analysis after 72 hr treatment. The cultures treated with 0.2 μg/mL were processed for cytochemical reaction, electron, confocal microscopical analyses, and for mtDNA molecular studies after 3 weeks' treatment; AZT was added to flasks or coverslips 3 times/week. For mtDNA analysis and biochemical analyses, the myotubes grown in flasks were purified by 9000 rpm centrifugation in Percoll gradient. Untreated flasks or coverslips were followed concurrently as controls and all the experiments were performed at least three times.

2.2. Electron microscopy analysis

Untreated and AZT cells treated for three weeks were pelletted and then fixed in 2.5% glutaraldehyde-Na-cacodylate buffer (Merck) (0.1 M, pH 7.2) at 4° for 2 hr, rinsed in the same buffer, and post-fixed in 1% OsO_4 Na-cacodylate buffer. The same protocol was applied on untreated and treated cells grown on coverslips.

The cells were dehydrated and embedded in epoxy resine and sectioned by ultramicrotome. Semifine sections (0.5 μm) were stained with toluidine blue and observed by light microscopy; ultrathin sections (80 nm) contrasted with uranyl acetate and lead citrate were examined by transmission electron microscope (Zeiss EM 10).

2.3. Cytochemical analysis for the succinate deydrogenase (SDH) and cytochrome oxidase (COX)

Control and cells treated with zidovudine for three weeks were fixed in 1% formaline for 5 min. For SDH staining, 2 mM nitroblue tetrazolium (NBT, Sigma) was added to 50 mL of 0.1 M phosphate buffer at pH 7.8, and mixed with 50 mL of 50 mM sodium succinate (ICN Biochemicals). Finally, 0.1 mM phenazine methosulphate (PMS, Sigma) was added. The reaction was performed for 30 min at 37°.

For COX staining, the reaction was performed for 20 min in incubation medium containing 0.2 M *p*-amino-diphenylamine (Sigma) and 0.2 M 1-hydroxy-2-naphthoic acid (Sigma) dissolved in 100% ethanol (BDH). This solution was added, together with cytochrome *c* (Fluka) (0.26 M final concentration) to Dulbecco's modified Eagle's medium (DMEM).

For the SDH and COX analyses, about 1000 cells from control and treated cells were scored at 100X with the microscope Leitz (Orthoplan). Statistical analysis was performed by χ^2 test.

2.4. Mitochondrial transmembrane potential

2.4.1. Isolation of mitochondria from skeletal muscle

The mitochondria were isolated from male Wistar rats. Briefly, tissue was removed, minced, and digested with Nagarase (5 mg/g, Subtilisin, ICN) for 10 min. The sample was diluted in ice-cold homogenization medium containing: 0.3 M sucrose, 1 mM EGTA, 5 mM MOPS, 5 mM KH_2PO_4, 0.1% bovine serum albumin (fatty acid-free), adjusted to pH 7.4, then transferred to a precooled glass homogenizer, resuspended (1 g/2 mL of homogenization medium), and homogenized. The homogenate was centrifuged twice at 1000 × *g* for 10 min (5°) and the supernatant was centrifuged at 10,000 × *g* for 10 min. The mitochondrial pellet was resuspended in 1.5 mL of homogenization medium.

2.4.2. Mitochondrial transmembrane potential on isolated mitochondria

Mitochondrial suspensions were incubated in medium [110 mM KCl, 75 mM mannitol, 20 mM MOPS, 10 mM glutamate, 1 mM malate, 1 mM EGTA, albumin 1 mg/mL (pH 7.0–7.2)] for 1 min at room temperature in the dark with JC-1 (1.5 μg/mg protein) in a final volume of 1 mL. At the end of incubation, the sample was analysed with a Coulter Epics XL (Coulter Corp.) flow cytometer, by measuring fluorescence intensity in the FL1 and FL2 channels with band-pass filters centred at 525 nm and 575 nm, respectively. Fluorescence compensation was performed, as previously reported [23]. AZT (0.4, 0.8, or 2 mg/mL) was added and the samples were analysed immediately. Statistical significance analysis was carried out by Student's *t*-test.

2.4.3. Mitochondrial transmembrane potential on myotubes

Coverslips of treated and untreated cells were washed with PBS and incubated for 20 min at 37° with the fluorescent JC-1 probe (1 μg/mL, Molecular Probes) dissolved in the incubation buffer (142 mM NaCl, 2.4 mM KCl, 1.2 mM K_2HPO_4, 1 mM $MgSO_4$, 10 mM HEPES, 1.2 mM $CaCl_2$, and 10 mM glucose). This dye, at low mitochondrial membrane potential, emits a green fluorescence, while at higher membrane potential, JC-1 forms red fluorescent "J-aggregates" [24,25]. The myotubes were examined with a Nikon PCM2000 Confocal Microscope System equipped with a Nikon Diaphot 300 inverted microscope and a 40X (1.3 NA) Nikon oil Fluor objective. The 488-nm Argon laser line was directed to the sample with single mode fiber optic cable, via high-precision laser coupler and through a 488/543 nm excitation filter. Pinhole size was set at 20 μm. Fluorescence emission light was passed back through a first dicroic mirror and divided by a second dicroic mirror into light emission higher or lower than 565 nm. Green emission fluorescence was collected through a BA 515/530 nm filter. Red emission fluorescence was passed through a BA 590/660 nm filter. The image size was set at 1024 × 1024 pixels. Laser line intensity, photometric gain, photomultiplier setting, filter attenuation, and pinhole size were kept rigorously constant throughout all the experiments. Confocal images were processed by an Image Analysis System Zeiss (Jena) KS 300 for evaluation.

In order to discriminate mitochondria on the whole profile of myotubes, segmentation was interactively performed referring to the Hue, Lightness and Saturation (HLS) colour model. The HLS thresholds were interactively modified to obtain a binary image suitable to automatic measurements. Assuming that red structures (JC-1 aggregates) are energized mitochondria and green structures (JC-1 monomers) are mitochondria not energized, two HLS intervals were defined, red and green mitochondria area % were measured, and red/green area % ratios were evaluated. All the above-mentioned steps were recorded in a macro function, which was automatically applied to all the images of the experiments.

Semiquantitative analysis was performed both in control and in treated myotubes. Typically, three cells were analysed in each field and at least 10 fields were considered. Data analysed were from four independent experiments. Statistical significance analysis was carried out by Student's *t*-test.

2.5. Biochemical analysis

2.5.1. Respiratory activity of isolated mitochondria

The oxygen consumption rate (QO_2) was determined polarographically using a Clark oxygen electrode (Gilson) in a water-jacketed chamber (1 mL). Measurements were made at 25° in a medium containing: 110 mM KCl, 75 mM mannitol, 20 mM MOPS, 10 mM glutamate, 1 mM malate,

1 mM EGTA, albumin 1 mg/mL (pH 7.0–7.2). After measuring the basal QO_2 with NADH + H^+ producing substrates, ADP (0.1 μM) was added. After ADP was depleted, QO_2 was measured in the presence of rotenone (8 μM), succinate (5 mM), antimycin (75 μM), ascorbate (1.87 mM), and *N*,*N*,*N*′,*N*′-tetramethyl-*p*-phenylendiamine (TMPD, 1.5 mM) and KCN (5 mM).

2.5.2. Mitochondrial enzyme activities on isolated mitochondria and myotubes

Mitochondrial complex I (NADH:ubiquinone reductase) activity was measured spectrophotometrically [26] at 30°. The reaction mixture contained in a final volume of 1 mL: 20 mM potassium phosphate, pH 7.5, 100 μM NADH, 1 mM KCN. The reaction was started by the addition of 50 mM ubiquinone-1 and read at 340 nm against a blank containing all the components except the starter. After 2 min, rotenone 10 μM was added to inhibit complex I and the inhibited rate observed for a further 5 min. The rotenone-sensitive rate was calculated by subtracting the rotenone-inhibited rates from the ubiquinone-stimulated rate.

Mitochondrial complex II (succinate:ubiquinone reductase, SDH) activity was assayed spectrophotometrically [27] at 30° and followed for 6 min. The reaction mixture contained, in a final volume of 1 mL: triethanolamine/HCl buffer 100 mM, pH 8.3, 0.5 mM EDTA, 2 mM KCN, 2 mM iodonitrotetrazolium chloride, 1% dimethyl sulfoxide. The reaction was started by the addition of 20 mM succinate and read at 500 nm against a blank containing all components except the starter.

Complex IV (cytochrome *c* oxidase, COX) activity was measured spectrophotometrically [28] at 30° and followed for 1 min. The reaction mixture contained, in a final volume of 1 mL: 0.2 M Tris–HCl buffer, pH 7, 0.001% lauryl-D maltoside. The reaction was started by the addition of 56 μM reduced cytochrome *c* and read at 550 nm against a blank containing 0.2 M Tris–HCl buffer, pH 7, 0.001% lauryl-D maltoside, 56 μM reduced cytochrome *c*, and 10 μM potassium ferricyanide.

The activity of citrate synthase was measured [29] following the formation of 5-thio-2 nitrobenzoate from acetylcoenzyme A and 5,5′-dithiobis2-nitrobenzoicacid (DTNB) at 412 nm (30°).

Protein concentration was assayed spectrophotometrically following the method of Lowry *et al*. [30] modified by Schacterle and Pollak [31].

Data were analysed by the analysis of variance (ANOVA) and Student's *t*-test for paired comparisons.

2.6. Molecular analysis of mtDNA

2.6.1. mtDNA depletion

Total DNA was prepared, from untreated and AZT treated cells, according to the method of Maniatis [32]. To investigate mtDNA depletion, 18s rDNA was chosen as internal standard to correct differences in the DNA loaded in each line. 18s rDNA and mtDNA are present in an almost similar number of copies in a cell, so they develop on the hybridized filters at about the same time. Five micrograms of total DNA was digested with *XhoI* (2 U/μg DNA) and electrophoresed through a 0.8% Seakem Gold Agarose gel. After capillary transfer to Z-probe GT membrane (Bio-Rad), the filters were hybridized with two specific probes both generated by PCR, gel-purified, checked with restriction enzymes, and labeled with digoxigenin by random priming (Dig-DNA Labeling and Detection Kit, Boehringer Mannheim). The first was the d-loop sequence, a highly conserved region of mtDNA, and the second the *18s* gene. Prehybridization, overnight hybridization, and washing were performed at 68°. The probes were detected by an anti-digoxigenin alkaline-phosphatase-conjugated antibody and the filters were developed for about 3 hr. Digitalized images of the bands were by a UMAX Power Look II™ scanner (UMAX Data System) and densitometric analysis was performed on a Macintosh computer using the public domain NIH-Image program (developed at the U.S. National Institutes of Health and available on the Internet at *http://rsb.info.nih.gov/nih-image*) with the aid of the bundled gel plotting macros. The d-loop/18s rDNA ratios were calculated and compared by Student *t*-test analysis.

2.6.2. mtDNA deletion

For the analysis of mtDNA deletions, Southern blot analysis was performed on 5 regions of mtDNA amplified by PCR reaction: fragment 1 5325 bp (L7721: GAC AAC AAA TCT CCA CAA TG; H13046: AGT AAT TAG TGG GGA GTA TC); fragment 2 "long" 16004 bp (P274: AAG CTA GTA CCT CTC AGG GTT GG; P16278: GAG GGT AGG CAA GTA AAG AGG G); fragment 3 7750 bp (P1045: AAA GCA TCT GGC CTA CAC CC; P8794: GGT GGC CTT GGT ATG TTC CT); fragment 4 5496 bp (P12962: CGC CAC ATC CAT AAC TGC T; P2157: GCT CCA TAG GGT CTT CTC GT); fragment 5 655 bp (P117: ACA GGC ATC TGG TTC TTA CT; P15762: CAT GTG TAA TCT TAC CTC CA). PCR amplifications were performed in 100-μL reaction mixtures containing PCR buffer II 1X (Perkin Elmer), 200 μM dNTPs, 500 nM primers, and 500 ng of total DNA. The PCR products were analysed both in gel electrophoresis and by Southern blot, as previously described.

2.7. Atomic force microscope (AFM) analysis

Aliquots of ethanol solution of cardiolipin (Sigma) were dried by evaporation under gentle jet of N_2. The dried powder was then re-hydrated in water in the absence and in the presence of 5 μM AZT and suspended by sonication. Under these conditions, large crystalline structures are formed; the concentration of AZT used apparently does not interfere with the formation of these crystals. A drop of suspension was placed on a freshly cleaved mica surface

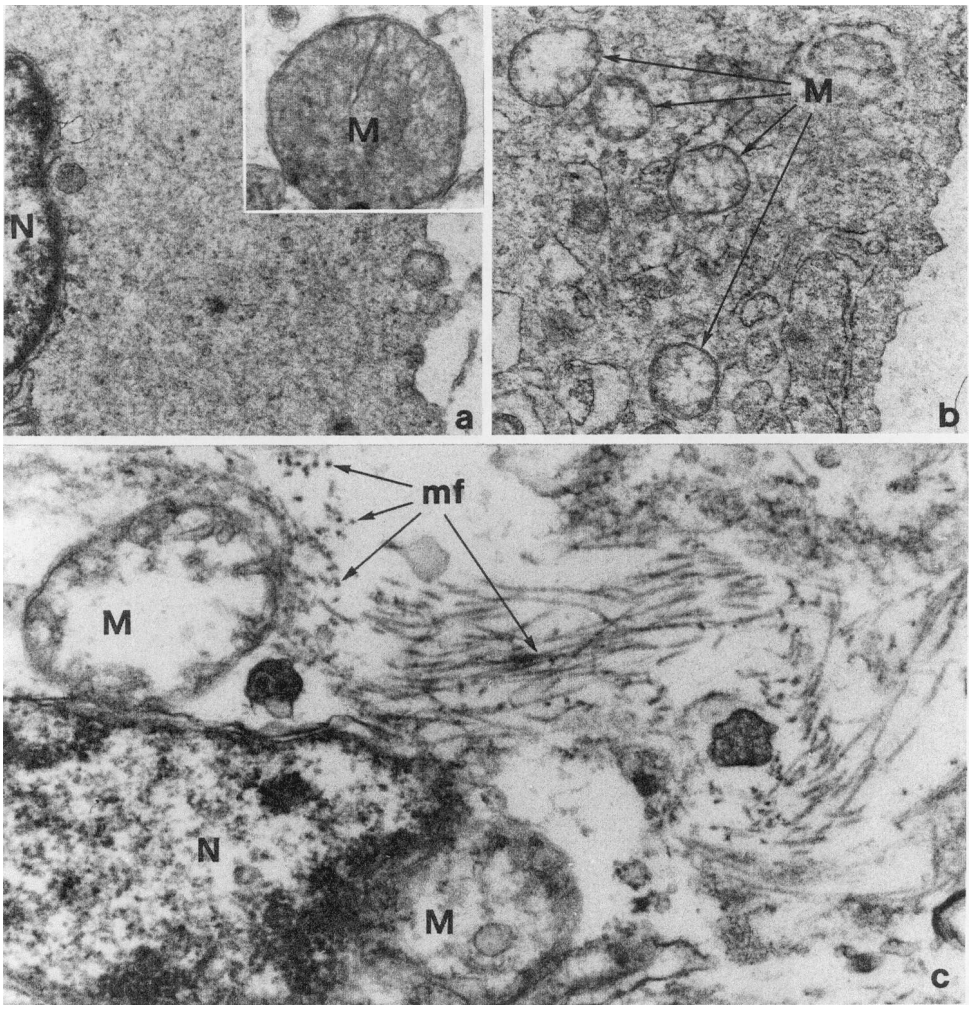

Fig. 1. Some ultrastructural aspects of control and three-week AZT-treated myotubes. (a) Low magnification of a normal myotube: around the nucleus, many scattered myofilaments and some mitochondria are observable. N, nucleus. Magn. 25.100X. In the insert at the higher magnification, a normal mitochondrion with a medium electron dense matrix and lamellar cristae is appreciable (M). Magn. 43.000X. (b) In the low magnification electron micrograph of an AZT-treated myotube, scattered myofilaments and some swollen mitochondria (M) are detectable. In the high magnification electron micrograph (c), myofilaments (mf) transversally, obliquely, and longitudinally sectioned and two swollen mitochondria (M) with few peripheral cristae are clearly visible. N, nucleus. Magn. 47.000X.

and the crystals observed by AFM (Digital Instruments Nanoscope III Multimode) working in tapping mode [33].

3. Results

3.1. Morphological and cytochemical observations

Morphological and cytochemical effects were investigated during 3-week AZT treatment. After a 2-week treatment, examination by phase-contrast microscopy showed that myotubes assumed a long and spindle-shaped morphology, as compared to untreated control cells. Moreover, functional alterations were also observed since the spontaneous contraction was abolished during the first week of long-term AZT treatment, and after 48 hr in short-term AZT treatment (data not shown).

The swelling of mitochondria was observed in myotubes only after three weeks of AZT treatment by electron microscopy. These organelles showed a very light matrix in which different size vescicules, probably representing residual cristae, were observable. Typical aspects of such ultra structural modifications are shown in Figs. 1 and 2.

Cytochemical analysis of SDH and COX activities showed a statistically significant decrease ($P < 0.01$) in the number of SDH-positive cells, as compared to untreated myotubes, after 48-hr AZT treatment, and after long-term AZT treatment. In contrast, no differences between treated and untreated cells were observed after the COX cytochemical staining.

3.2. Mitochondrial transmembrane potential

Alterations of the mitochondrial energy transducing mechanism were previously observed *in vivo* and *in vitro* by

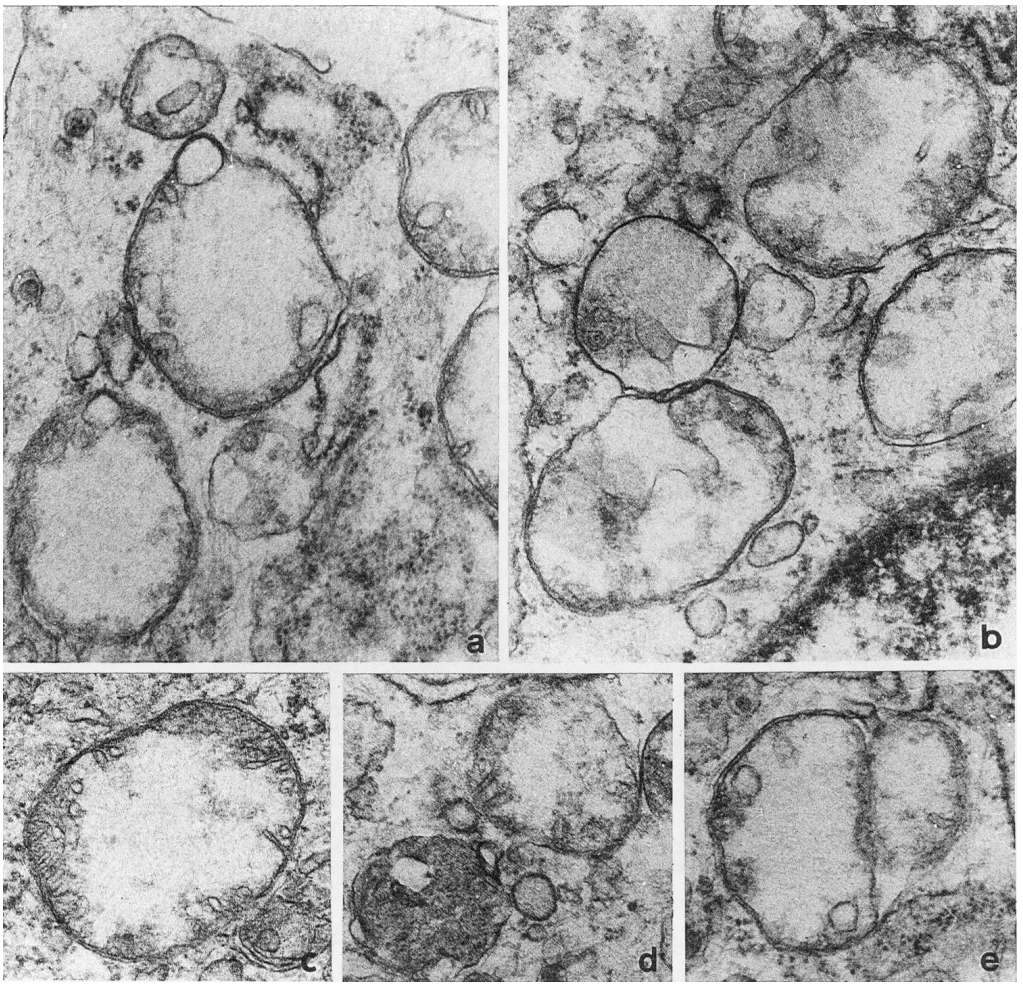

Fig. 2. A wide variety of mitochondrial modifications in the three-week AZT-treated myotubes, all characterized by a swollen appearance of the organelles, is shown. (a) Vescicular residues of cristae; (b) widening of external camera; (c) small tubular and/or vescicular peripheral cristae; (d) medium-dense matrix residuals; (e) inner membrane dividing a mitochondrion into two compartments; in the right compartment a smaller mitochondrion-like structure is observable. Magn. 43.000X.

measuring the mitochondria electrical transmembrane potential ($\Delta\Psi$) [9]. In this work, the analysis of the mitochondrial transmembrane potential was performed in isolated muscle mitochondria and in living cells with JC-1 and analysis by flow cytometry and by laser-scanning confocal microscopy, respectively.

3.2.1. Mitochondrial transmembrane potential on isolated mitochondria

Fig. 3a shows a typical image obtained from control mitochondria incubated for 1 min with JC-1. The flow cytometric analysis revealed that immediate addition of AZT (0.8 mg/mL) caused an alteration in mitochondrial transmembrane potential (Fig. 3b) in about 55% of the total mitochondrial population. A 40% decrease ($P < 0.01$) in the FL2/FL1 ratio was observed, as compared with the control samples. Similar results were obtained with 0.4 and 2 mg/mL of AZT (not shown).

3.2.2. Mitochondrial transmembrane potential on myotubes

Control myotubes (Fig. 4a) preferentially displayed red fluorescence, indicating that a high fraction of mitochondria are in the energized state. Myotubes treated with the higher

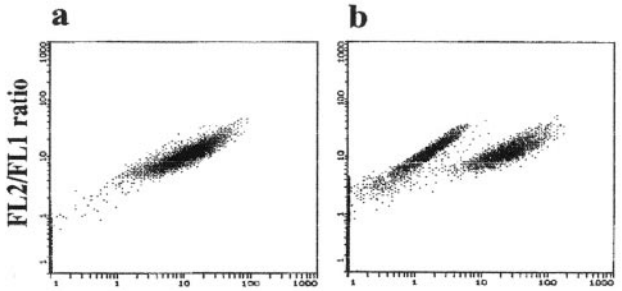

Fig. 3. Cytofluorimetric analysis of membrane potential changes, in muscle-isolated mitochondria stained with JC-1 in (a) control and (b) AZT-treated sample (0.8 mg/mL, 1 min). Data are expressed as the ratio of JC-1 fluorescence intensity of FL2/FL1 channels.

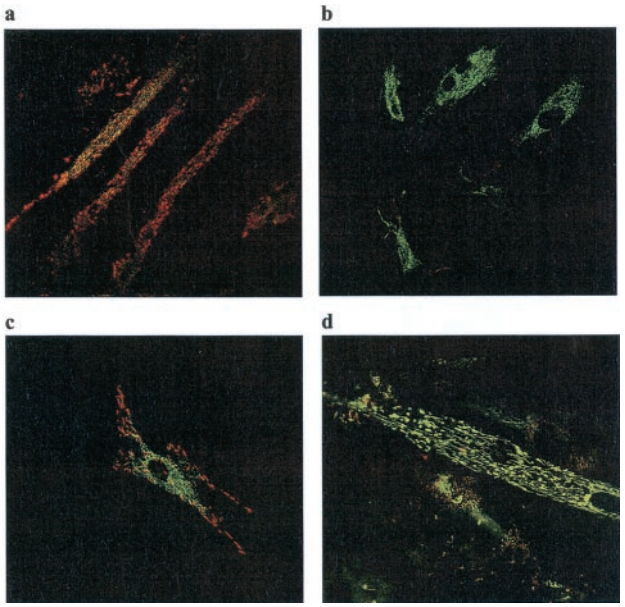

Fig. 4. Confocal images of myotubes stained with JC-1 (a) prior to treatment; (b) after 72-hr AZT (2 mg/mL) treatment; (c) 72 hr following the end of AZT (2 mg/mL) treatment; and (d) after AZT (0.2 μg/mL) three-week treatment.

dose of AZT showed no effect after 4 and 24 hr. Alterations in mitochondrial energy transduction were observed after 48 hr, whereas 100% green fluorescence after 72-hr treatment was detected (Fig. 4b). This effect was found to be reversible, since 72 hr following the end of AZT treatment, the analysis of the red/green ratios showed that about 62% of mitochondria returned to the energized state (Fig. 4c). The long-term AZT-treated myotubes (Fig. 4d) displayed a predominant green fluorescence, indicating the presence of high proportion of depolarized mitochondria. Fig. 5 shows the magnitude of the shift, expressed as the red/green fluorescence ratio for long-term AZT-treated cells, as compared to untreated control cells; the red fluorescence was lost by

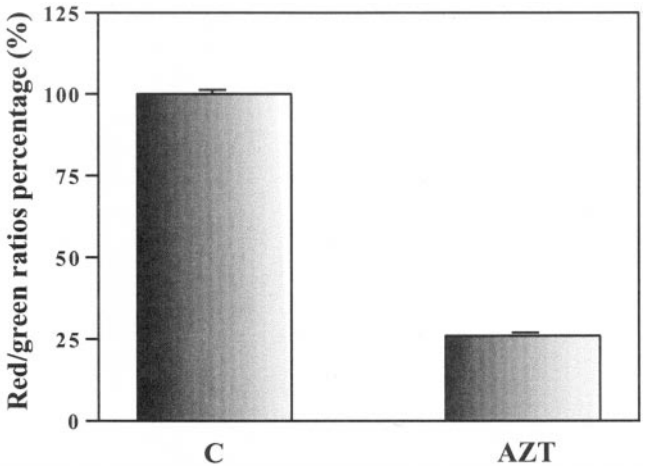

Fig. 5. Changes in the red/green fluorescence ratios for untreated and three-week AZT-treated myotubes.

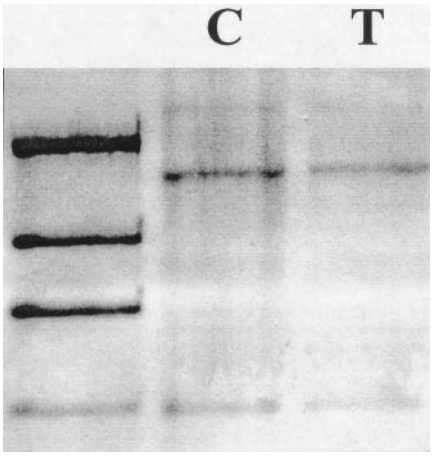

Fig. 6. Effect of AZT on mtDNA depletion in myotube cultures. Southern blot of extracted DNA from control myotubes (C) and myotubes treated for three weeks with 0.2 μg/mL of AZT (T). From top to bottom: linearized mtDNA, 18s rDNA. Mobility of standard molecular weight indicated on the left. Results shown are from one out of five independent experiments.

about 74%. Statistical analysis demonstrated that the AZT response was highly significant ($P < 0.01$).

3.3. Biochemical analysis

3.3.1. Oxygen consumption and enzyme activity of isolated mitochondria

The oxygen consumption rate increased 4-fold in the presence of ADP. AZT (0.8 mg/mL) caused a slight decrease in QO_2. The SDH activity decreased to 42% of control value ($P < 0.04$) when measured polarografically and to 49% of control value when measured spectrophotometrically. AZT at the concentration of 0.4 mg/mL was not effective; at 2 mg/mL it decreased SDH activity to 39%. The COX activity was never altered.

3.3.2. Enzyme activity of myotubes

The biochemical analyses were performed after 48 hr and three-week AZT treatments. The activities of NADH-dehydrogenase, COX, and citrate synthase were not affected (data not shown). However, biochemical analyses showed a statistically significant decrease ($P < 0.05$) of SDH activity both in short- (5.21 ± 0.52) and long-term treatments (6.88 ± 0.86), if compared to the control (8.69 ± 0.39).

3.4. Molecular analysis of mtDNA

The mtDNA depletion caused by AZT treatment was investigated by treating myotubes for three weeks (0.2 μg/mL) or 72 hr (2 mg/mL). Fig. 6 shows the Southern blot analysis of DNA extracted from control and long-term AZT-treated myotubes. Densitometric analyses of the labelled bands revealed a decrease in mtDNA in treated myotubes. The difference between the treated and untreated

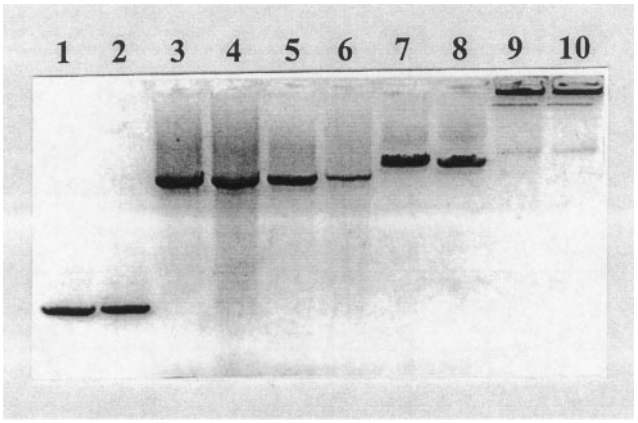

Fig. 7. Effect of AZT on mtDNA deletions in myotubes cultures. Gel electrophoresis of five regions of mtDNA amplified by PCR reactions from control myotubes and myotubes treated for three weeks with 0.2 μg/mL of AZT. Results shown are from one out of five independent experiments. Lanes 1, 3, 5, 7, and 9: regions from mtDNA in control myotubes; lanes 2, 4, 6, 8, and 10: regions from mtDNA in AZT-treated myotubes.

samples was about 40% ($P < 0.05$). No effect was detected after short-term treatment AZT.

To investigate the presence of deletions in mtDNA in long-term treated myotubes, the entire molecule was evaluated. The migration patterns of PCR products shows the absence of deletions in AZT-treated myotubes (Fig. 7). The data were confirmed by Southern blot analysis.

3.5. Atomic force microscopy (AFM)

In order to investigate whether the effect of AZT on membrane potential may be related to a modification of the membrane physico-chemical properties, the effect of AZT was investigated on cardiolipin liquid-crystalline structure. In Fig. 8 are shown the images of the structure of cardiolipin after AZT treatment (Fig. 8b), with respect to the control (Fig. 8a). The presence of large crystals could be observed in both samples. In the case of pure cardiolipin, molecular details inside the crystals were seen (Fig. 8a). Interestingly, in the presence of AZT, no molecular order could be found (Fig. 8b).

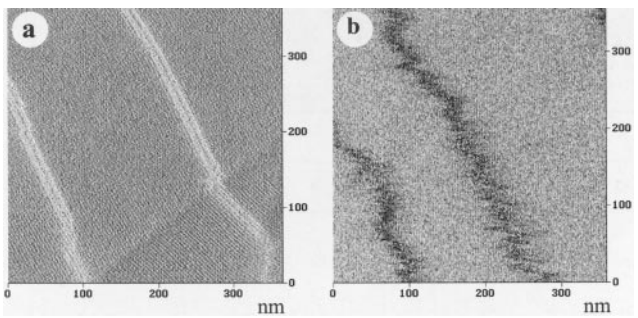

Fig. 8. AFM images of (a) cardiolipin hydrated in H_2O and (b) cardiolipin hydrated in H_2O plus 5 μM AZT. The images were obtained by Tapping Mode in air and the diagonal lines visible in both images indicate steps of large crystals.

4. Discussion

The present study shows that AZT significantly induced: (i) mitochondrial membrane potential alterations in isolated mitochondria; (ii) mitochondrial membrane potential alterations in myotubes, associated with a block of the spontaneous contractions of myotubes, both in short- and long-term treatments; and (iii) morphological mitochondrial alterations and mtDNA depletion in long-term treatment. In particular, rat muscle cells exposed to clinically relevant concentrations of AZT for three weeks showed changes of mitochondria at the morphological, biochemical, and molecular level. At the ultrastructural level, it has been observed in rat myotubes that the mitochondria damage proceeds through a series of stages towards a mitochondrial disruption. The early change observed is a dilution of the matrix material as shown by the decrease in its electron density. It has been suggested that ultrastructural modifications are related to alterations in mtDNA, as a consequence of the inhibitory effect of AZT on DNA polymerase γ [7,34]. The depletion of mtDNA was observed in muscle biopsies of treated patients [13] and of treated rats with AZT [7,9]. On the other hand, no change in mtDNA amount between AZT treated and untreated human or mouse cultured muscle cells was detected [12,21]. In contrast, in rat myotubes we observed a significant depletion of mtDNA (about 40%) after long-term, but not after short-term treatment.

In agreement with the results obtained by Southern blot analysis in human samples and in cultured human muscle cells [13,20,21,35], no deletions were detected by PCR amplifications of entire mtDNA after long-term AZT treatment in rat myotubes.

The inhibition in mitochondrial energetic functions was shown in human studies [20,36,37], in animal model systems [8,18], and in mitochondria isolated from rat skeletal muscle, brain and liver [18]. Alterations in energy transducing mechanisms were previously observed by measuring the electrical transmembrane potential ($\Delta\Psi$) of muscle mitochondria of long-term AZT-treated rats; these membrane potential abnormalities closely resemble those of mitochondria in the presence of externally added AZT [9].

Using the fluorescent dye JC-1, an effective probe for detecting rapid changes in mitochondrial activity, we provide the first direct evidence in living cells that AZT induces alterations in the mitochondrial transmembrane potential, even after a short-term treatment. This result was also confirmed in isolated muscle mitochondria stained with JC-1 and analysed by flow cytometry.

The respiratory chain enzymes have been studied in muscle from AZT-treated AIDS patients [20,38], in long-term AZT-treated rats [39], and in human cell lines [17,21], with contrasting results. We have observed no modifications in citrate synthase, cytochrome *c* oxidase, or NADH deydrogenase activities. At variance with the above enzymatic activities, the SDH was decreased by short- (about 40%)

and long-term (about 21%) AZT treatments; these data were also confirmed by cytochemical analysis. A similar reduction in SDH activity (about 49%) was also observed in isolated mitochondria, while no modifications in COX activity were detected. The decrease in SDH activity, an enzyme totally codified by nuclear DNA and the changes in membrane potential after short-term treatment, demonstrate that AZT may induce a significant and immediate effect on mitochondrial energy metabolism, independent of mtDNA depletion. The consequent energetic abnormalities may explain the block of spontaneous contractions of cultured myotubes observed at this time.

The effect of AZT on membrane potential as well as on the SDH may be related to a modification of the membrane physico-chemical properties consequent to a perturbation caused by AZT on the elementary structure of the membrane. This possibility is suggested by the results of a study with AFM on liquid-crystalline organization of cardiolipin. This phospholipid was chosen to construct the crystalline model because of its high concentration in the inner mitochondrial membrane as well as in view of its absolute requirement for some mitochondrial enzyme activities [40]. The AFM observations show that the presence of AZT hinders the regular aggregation of cardiolipin molecules by interacting with the hydrophobic driving force (a detailed report of this effect is in preparation). The lack of changes in COX activity, which is dependent on cardiolipin, is rather puzzling. However, the cardiolipin pool required for the optimal functioning of this enzyme complex is strictly located in the lipidic annulus surrounding the protein and may be perturbed only by very drastic interactions (e.g. interactions leading to peroxidation of cardiolipin). In conclusion, the early changes induced by AZT on some mitochondrial properties reported by Modica-Napolitano [18], our previous observations regarding the effect of addition of AZT on mitochondrial membrane potential [9], and the present data indicate that there are two effects by AZT on mitochondria: (i) a short-term reversible effect regarding only some bioenergetic parameters; and (ii) a long-term effect also involving the synthesis of mtDNA. The short-term effect seems to essentially affect parameters depending on the physico-chemical properties of mitochondrial membrane such as membrane potential and osmotic equilibrium.

Acknowledgments

This study was supported in part by Telethon project no. 46. We would like to thank Professor U. Muscatello for helpful discussion and critical reviewing of the manuscript and R. Melli for preparing figures and editorial assistance.

References

[1] Hao Z, Cooney DA, Hartman NR, Perno CF, Fridland A, De Vico AL, Sarngadharan MG, Broder S, Johns D. Factors determining the activity of 2′,3′-dideoxynucleosides in suppressing human immunodeficiency virus in vitro. Mol Pharmacol 1988;34:431–5.

[2] Bessen LJ, Greene JB, Louie E, Seitzman P, Weinberg H. Severe polymyositis-like syndrome associated with zidovudine therapy of AIDS and ARC. N Engl J Med 1988;318:708.

[3] Dalakas MC, Illa I, Pezeshkpour GH, Laukaits JP, Cohen B, Griffin JL. Mitochondrial myopathy caused by long-term zidovudine therapy. N Engl J Med 1990;322:1098–105.

[4] Gertner E, Thun JR, Williams DN, Simpson M, Balfour HH, Rhame F, Henry K. Zidovudine-associated myopathy. Am J Med 1988;86:814–8.

[5] Gorard DA, Henry K, Giloff RJ. Necrotising myopathy and zidovudine. Lancet 1988;1:1050.

[6] Helbert M, Fletcher T, Peddle B, Harris JR, Pinching AJ. Zidovudine-associated myopathy. Lancet 1988;2:689–90.

[7] Lewis W, Gonzalez B, Chomyn A, Papoian T. Zidovudine induces molecular, biochemical and ultrastructural changes in rat skeletal muscle mitochondria. J Clin Invest 1992;89:1354–60.

[8] Lamperth L, Dalakas MC, Dagani F, Anderson J, Ferrari R. Abnormal skeletal and cardiac muscle mitochondria induced by zidovudine (AZT) in human muscle *in vitro* and in an animal model. Lab Invest 1991;65:742–51.

[9] Masini A, Scotti C, Calligaro A, Cazzalini O, Stivala LA, Bianchi L, Giovannini F, Ceccarelli D, Muscatello U, Tomasi A, Vannini V. Zidovudine-induced experimental myopathy: dual mechanism of mitochondrial damage. J Neurol Sci 1999;166:131–40.

[10] De la Asuncion JG, Del Olmo ML, Sastre J, Millan A, Pellin A, Pallardo FV, Vina J. AZT treatment induces molecular and ultrastructural oxidative damage to muscle mitochondria. J Clin Invest 1998;102:4–9.

[11] Semino-Mora MC, Leon-Monzon ME, Dalakas MC. The effect of L-carnitine on the AZT-induced destruction of human myotubes. Part II: treatment with L-carnitine improves the AZT-induced changes and prevents further destruction. Lab Invest 1994;71:773–81.

[12] D'Amati G, Lewis W. Zidovudine causes early increases in mitochondrial ribonucleic acid abundance and induces ultrastructural changes in cultured mouse muscle cells. Lab Invest 1994;71:879–84.

[13] Arnaudo E, Dalakas M, Shanske S, Moraes CT, Dimauro S, Shon EA. Depletion of muscle mitochondrial DNA in AIDS patients with zidovudine-induced myopathy. Lancet 1991;337:508–10.

[14] Simpson MV, Chin CD, Keilbaugh SA, Lin T, Prusoff H. Studies on the inhibition of mitochondrial DNA replication by 3′-azido-3′-deoxythymidine. Biochem Pharmacol 1989;38:1033–6.

[15] Hobbs GA, Keilbaugh SA, Simpson MV. The Friend murine erythroleukemia cell, a model system for studying the association between bone marrow toxicity induced by 3′-azido-3′-deoxythymidine and dideoxynucleoside inhibition of mtDNA replication. Biochem Pharmacol 1992;43:1397–400.

[16] Hayakawa M, Ogawa T, Sugiyama S, Tanaka M, Ozawa T. Massive conversion of guanosine to 8-hydroxyguanosine in mouse liver mitochondrial DNA by administration of azidothymidine. Biochem Biophys Res Commun 1991;176:87–93.

[17] Benbrik E, Chariot P, Bonavaud S, Ammi-Said M, Frisdal E, Rey C, Gherardi R, Barlovatz-Meimon G. Cellular and mitochondrial toxicity of zidovudine (AZT), didosine (ddI) and zalcitabine (ddC) on cultured human muscle cells. J Neurol Sci 1997;149:19–25.

[18] Modica-Napolitano JS. AZT caused tissue-specific inhibition of mitochondrial bioenergetic function. Biochem Biophys Res Commun 1993;194:170–7.

[19] Barile M, Valenti D, Quagliariello E, Passarella S. Mitochondria as cell targets of AZT (zidovudine). Gen Pharmacol 1998;31:531–8.

[20] Mhiri C, Baudrimont M, Bonne G, Geny C, Degoul F, Marsac C, Roullet E, Gherardi R. Zidovudine myopathy: a distinctive disorder associated with mitochondrial disfunction. Ann Neurol 1991;29:606–14.

[21] Herzberg NH, Zorn I, Zwart R, Portegies P, Bolhuis PA. Major growth and minor decrease in mitochondrial enzyme activity in cul-

tured human muscle cells after exposure to zidovudine. Muscle Nerve 1992;15:706–10.
[22] Pinset C, Montarras D. Cell system for *ex vivo* studies of myogenesis: a protocol for the isolation of stable muscle cell population from newborn to adult mice. In: Celis JE, editor. Cell biology—a laboratory handbook. San Diego: Academic Press, 1994. p. 199–206.
[23] Cossarizza A, Ceccarelli D, Masini A. Functional heterogeneity of an isolated mitochondrial population revealed by cytofluorimetric analysis at the single organelle level. Exp Cell Res 1996;222:84–94.
[24] Smiley ST, Rees M, Mottola-Hartshorn C, Lin M, Chen A, Smith TW, Steel GD, Chen LB. Intracellular heterogeneity in mitochondrial membrane potentials revealed by a J-aggregate-forming lipophilic cation JC-1. Proc Natl Acad Sci USA 1991;88:3671–5.
[25] Troyan MB, Gilman VR, Gay CV. Mitochondrial membrane potential changes in osteoblasts treated with parathyroid hormone and estradiol. Exp Cell Res 1997;233:274–80.
[26] Ragan CI, Wilson MT, Darley-Usmar MV, Lowe PN. Subfractionation of mitochondria, and isolation of the proteins of oxidative phosphorylation. In: Darley-Usmar UM, Richwood D, Wilson MT, editors. Mitochondria, a practical approach. London: IRL Press, 1987. p. 79–112.
[27] Munujos P, Coll-Canti J, Gonzales-Sastre F, Gella FJ. Assay of succinate deydrogenase activity by a colorimetric-continous method using iodonitrotetrazolium chloride as electron acceptor. Anal Biochem 1993;212:506–9.
[28] Wharton DC, Tzagoloff A. Cytochrome oxidase from beef heart mitochondria. Methods Enzymol 1967;10:245–50.
[29] Sugden PH, Newsholme EA. NAD^+-linked isocitrate dehydrogenase, glutamate dehydrogenase, aspartate aminotransferase and alanine aminotransferase in nervous tissues from vertebrates and invertebrates. Biochem J 1975;150:105–11.
[30] Lowry OH, Rosenbrough NJ, Farr AL, Randall RJ. Protein measurement with the Folin phenol reagent. J Biol Chem 1951;193:265–75.
[31] Schacterle GR, Pollak RL. A simplified method for the quantitative assay of small amounts of protein in biologic material. Anal Biochem 1973;51:654–5.
[32] Sambrok-Fritsch-Maniatis. Molecular cloning: a laboratory manual. New York: Cold Spring Harbor Laboratory Press, 1989.
[33] Zhong Q, Innis D, Kjoller K, Elings WB. Fractured polymer/silica fiber surfaces studied by tapping mode atomic force microscopy. Surf Sci Lett 1993;290:688–92.
[34] Lewis W, Papoian T, Gonzalez B, Louie H, Kelly DP, Payne RM, Grody WW. Mitochondrial ultrastructural and molecular changes induced by zidovudine in rat hearts. Lab Invest 1991;65:228–36.
[35] Casademont J, Barrientos A, Grau JM, Pedrol E, Estivill X, Urbano-Marquez A, Nunes V. The effect of zidovudine on skeletal muscle mtDNA in HIV-1 infected patients with mild or no muscle dysfunction. Brain 1996;119:1357–64.
[36] Dalakas MC, Leon-Monson ME, Bernardini I, Gahl WA, Jay CA. Zidovudine-induced mitochondrial myopathy is associated with muscle carnitine deficiency and lipid storage. Ann Neurol 1994;35:482–7.
[37] Weissman JD, Costanitinis I, Hudgins P, Wallace DC. ^{31}P magnetic spectroscopy suggested impaired mitochondrial function in AZT-treated HIV-infected patients. Neurology 1992;42:519–23.
[38] Chariot P, Gherardi R. Partial cytochrome *c* oxidase deficiency and cytoplasmic bodies in patients with zidovudine myopathy. Neuromuscular Disord 1991;1:537–63.
[39] Linnane AW, Degli Esposti M, Generowicz M, Luff AR, Nagley P. The universality of bioenergetic disease and amelioration with redox therapy. Biochim Biophys Acta 1995;1271:191–4.
[40] Tzagoloff A. Mitochondria. New York: Plenum Press, 1982.